International Journal of Energy Production and Management
https://www.acadlore.com/journals/IJEPM

Review on Heat Transfer Enhancement by Internal Obstructions in Enclosed Cavities under Natural Convection

Hussien Aziz Saheb[1*], Ahmed Kadhim Hussein[2]

[1] Mechanical Engineering Department, University of Babylon, College of Engineering, 00964 Diwaniya, Iraq
[2] Mechanical Engineering Department, University of Babylon, College of Engineering, 00964 Hilla, Iraq

[*] Correspondence: Hussien Aziz Saheb (eng419.hussien.aziz@student.uobabylon.edu.iq)

Received: 06-26-2025 **Revised:** 08-02-2025 **Accepted:** 12-16-2025

Citation: H. A. Saheb and A. K. Hussein, "Review on heat transfer enhancement by internal obstructions in enclosed cavities under natural convection," *Int. J. Energy Prod. Manag.*, vol. 11, no. 1, pp. 89–105, 2026. https://doi.org/10.56578/ijepm110107.

Abstract: This review of the current literature highlights the barriers present within cavities and their contribution to heat dissipation and cooling of various activities. This study shows a set of factors that affect the function of the obstacle (shape, length, size, thickness, and location of the obstacles). The variation in boundary conditions between obstacles and cavity walls has opened up broad horizons for scientific research in the field of heat transfer (HT) and fluid flow. Despite significant progress, research gaps remain. Most previous studies have focused on simple shaped obstacles within cavities with uniform boundaries. There is a distinct lack of studies exploring the effect of complex such as U/L/H shapes or orientable obstacles within complex cavities or under dynamic conditions such as non-uniform heating or varying magnetic fields. It was found that the Nusselt number increased by 15.56% depending on the shape of the internal obstacle, which gives an advantage to some obstacle shapes over others and highlights the importance of choosing the obstacle and cavity shape so that the best HT is obtained. This study is the first to compare simple and complex shapes of obstacles, and this is the innovative point of this review.

Keywords: Three dimensional; Hybrid nanofluid; Natural convection; Cavity; Obstacles; Nanofluid

1 Introduction

Convection inside cavities has received a great deal of study because it is fundamentally different from heat transfer (HT) on external surfaces, where boundary conditions play a pivotal role in controlling the heat transfer rate (HTR) and fluid flow inside closed cavities. This in turn leads to non-uniform heat distribution in a cavity, a fundamental challenge for researchers. The cavities are a promising field in many industrial applications. Rapid progress in the field of computing and simulation software has provided researchers with an opportunity to investigate HT and fluid flow in cavities and use complex boundary conditions and invent more complex shapes and different parameters to enhance HT performance [1].

The importance of obstacles inside cavities emerged with the emergence of the importance of heat convection and its consideration as a promising, clean and economical technique that can be exploited in electronic cooling and heat dissipation in various current industries [2]. In recent research, Rashid et al. [3] used a wavy channel to in enhance the HTR. Hashim et al. [4] studied HT through a wavy wall. Nasir et al. [5] examined inspected irreversibility phenomenon produced by thermal exchange in nano liquid flow past a radially flexible disk. Sadeghi et al. [6] investigated the effect of fins on HT performance.

Recently, nanofluids have attracted extensive research interest due to their exceptional HT properties and their potential exploitation in a wide range of possible applications, including: energy storage systems, HT enhancement, solar collectors, crystal growth in magnetically influenced cavities, Cooling electronic systems, nuclear reactors, metal cooling in open-surface reservoirs, technologies of biomedical [7], and automotive thermal control systems [8]. Li et al. [9] employed an artificial neural network (ANN) backpropagation technique, Amplified with the Bayesian regularization approach. Numerical simulations were carried out by Cherif et al. [10], to depict hydrothermal attributes generated by spinning heated obstacles fitted in triangular chamber. Role of gradients produced by buoyantly driven forces to enhance exchange in heat by placing obstruction in a chamber was revealed by Khan et

al. [11]. Abed et al. [12] investigated the effect of magnetic field (MF) on HT. Abdulsahib et al. [13]. Studied the effect of objects inside cavities on the HTR.

Minea [14] classified hybrid materials into three types based on electron orbitals and covalent bonding between polymerized silanol molecules. Turcu et al. [15] found that hybrid nanofluid enhance HT due to a synergistic effect compared to mono nanofluid. Huminic and Huminic [16] showed that hybrid nanoparticles, due to their improved physiochemical properties, offer better thermal performance and stability than single nanoparticles. Nasir et al. [17] mathematically analyzed hybrid nanofluid flow under mixed convection, considering radiative energy and nonlinear thermal effects over an exponential domain. Chamkha et al. [18] Surveyed natural convection (NC) in a semicircular cavity and this numerical study proved that the hybrid nanofluid enhances HT better than the conventional fluid. There are many excellent works that have been adopted for the purpose of benefiting from them in how to exploit hybrid nanofluids in various engineering and industrial applications [19].

The elements or objects inside cavities helps control HT by providing both passive and active HT, which contributes effectively to many applications in automotive, electronics, aerospace, vacuum and engineering systems [20]. Moukalled and Acharya [21] studied of the effect of a rotating solid body inside a closed cavity, as this body affected the formation of vortices and HT. Nasir et al. [22] tried to control the HTR of a nanofluid by introducing a magnetic field. Dutta et al. [23] found that the magnetic field inhibits HT. Nasir et al. [24] used computational to design a trihybrid nanofluid, show significant superiority in thermal properties compared to conventional fluids.

Saha [25] Investigate the effect of magnetic field on NC in a trapezoidal cavity filled with a nanofluid. Geridonmez and Oztop [26] examined the effect of crossed, partially guided magnetic fields on the hydrothermal performance of nanofluids in an enclosure, and reported a weakening in convective flow strength. Similarly, Alsabery et al. [27] analyzed the role of solid nanoparticle inclusion in enhancing thermal performance, attributing the improvement to the intensified magnetic field effects. Sreedevi and Reddy [28] assessed the effect of Brownian motion on HT.

Saravanan and Sivaraj [29] analyzed the interaction between thermal radiation and NC in a square cavity including a heat source. It was shown that with increasing the dimensions of the heat source, the HTR will improve, as heat convection increases in the upper part of the cavity while heat conduction dominates in the lower part of the cavity. Rahimi et al. [30] examined NC in a cavity filled with a nanofluid, and the effect of the internal heater position, as well as the Ra and nanofluid concentration, on HT and entropy generation was investigated. The results of this study showed that the heater position affects the fluid flow and the Nusselt number (Nu) increases with increasing nanofluid concentration and increasing Ra.

The effect of the upper wavy wall of a square cavity filled with a nanofluid analyzed by Uddin et al. [31], The results showed that the HT improved by 20% with increasing the Ra, wall number, and nanoparticle concentration, while it decreased with increasing the Hartmann number (Ha) and nanoparticle size. The wavy walls of the cavities increase NC but the increased number of waves reduces the Nu [32]. A study by Ismail et al. [33] showed that the presence of an obstacle within the cavity affects the fluid flow and creates a hydrodynamic obstruction.

Kalidasan and Kanna [34] studied NC in an L-shaped cavity and the effect of the presence of body inside the cavity filled with a hybrid nanofluid. Mohebbi and Rashidi [35] determined that the greatest HT occurs when the obstacle is located near the lower left corner of the cavity. Bouchoucha et al. [36] explored generation of entropy in cavity with a thick bottom wall and found that increasing the thickness of wall results in a reduction in generation of entropy.

Many studies have showed that increasing Ra significantly enhanced NC, leading to a higher Nu and increased HT efficiency [37]. In the work of Armaghani et al. [38], examined NC of a (Al_2O_3-H_2O) in an L-shaped cavity equipped with a baffle.

The current study aims to shed light on the obstacles and objects present inside cavities filled with different fluids. It shows that there is a lack in the experimental researches and a scarcity in comparisons between experimental and numerical results, as well as being limited only to conventional obstacle shapes (square, rectangular, cylinder, triangle, ..., etc.) without verifying more complex shapes. This is the research gap in this study.

This review uniquely covers recent studies from 2020 to 2025, proposes a new classification for obstacle shapes (simple vs. complex), analyzes contradictory findings in obstacle configurations, and presents a comparative discussion of Finite Element Method (FEM) and Finite Volume Method (FVM) approaches elements not addressed in previous reviews.

In the next part of the review, the review is structured based on the types of obstructions within the cavities.

2 Types and Classifications of Obstacles

2.1 Triangular Obstacles

Chatterjee et al. [39] studied NC of a (Al_2O_3-H_2O) in triangular cavity containing an inverted triangular hot obstacle. FEM was used. Parameters used, including Ra (10^3–10^6) and the size of obstacle. The results showed that the best HTR is achieved at the smallest obstacle size, smaller obstacle size means less obstruction to fluid

flow. Roshani et al. [40] studied NC of a (Al_2O_3-H_2O) in a triangular cavity containing obstacles inverted triangle. parameters such as Ra (10^3–10^5) was studied. This study proved that the obstacle enhanced HT and thus resulted in an increase in the Nu values. The obstacle within the cavity disrupts the streamline, creating local vortices. These vortices move the fluid better near hot and cold surfaces, reducing the thickness of the thermal boundary layer. Yaseen et al. [41] studied NC in triangular enclosure filled with a shear-thinning non-Newtonian fluid, Results showed that increasing Ra intensifies convection and improved ($N\bar{u}$). Lower power-law index (n) values, representing stronger shear-thinning behavior, lead to higher $N\bar{u}$ due to reduced viscosity. The best HT occurred when the obstacle was placed closest to the heated base (B = 0.2 H).

Mahmuda and Ali [42] studied NC of (Al_2O_3-H_2O) in a square cavity containing a centrally placed heat-conducting triangular obstacle. The influence of a transverse magnetic field was considered using the FEM. The effects of the Ra, Ha, and (ϕ) were investigated. Results indicated that the obstacle enhances fluid mixing and generates thermal vortices, leading to thinner thermal boundary layers and an increased Nu, thus enhancing HT. Increasing Ra strengthened convection, while higher Ha values suppressed flow intensity due to magnetic damping. Furthermore, adding nanoparticles enhanced thermal conductivity and improved the overall thermal performance of the system.

Maneengam et al. [43] used Generalized Finite Element Method (GFEM) to investigate the HT in a square cavity with a wavy bottom wall filled with a hybrid nanofluid inside which several obstacles of different shapes were placed. The study proved that the triangular obstacles provided the best HT, and that increasing the undulations and Ha reduces the HT efficiency. The triangular obstacles enhanced the Nu by 15.54%. The reason for this is that the triangular obstacles accelerate the fluid flow and increases the temperature gradient near the hot wall. The FEM is preferred in NC studies due to its accuracy and flexibility in handling complex geometries and boundary conditions. In contrast, the FVM, despite its strong conservation properties, faces challenges in such scenarios. As a result, most recent studies have adopted FEM as the primary modeling approach.

Table 1 presents an organized summary of the most prominent previous studies in terms of reference, researchers, mathematical model, working fluid, study parameters, geometry, physical model, as well as other aspects related to the subject of the study.

Table 1. Summary of the literatu rereview relatingtothe current work: triangular obstacles

Ref.	Researchers	Math. Model	Working Fluid	Study Parameters	Geometry	Physical Model
[39]	Chatterjee et al.	FEM	Al_2O_3–H_2O	$10^3 \leq Ra \leq 10^6$; $0 \leq Ha \leq 70$; $0^\circ \leq \gamma \leq 180^\circ$	Isosceles triangular cavity with an inverted triangular hot obstacle.	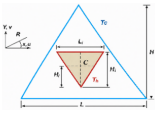
[40]	Roshani et al.	FEM	Al_2O_3–H_2O	$10^3 \leq Ra \leq 10^5$	Triangular cavity with a centrally placed triangular cylinder.	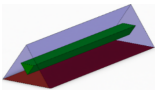
[41]	Yaseen et al.	LBM	Non-Newtonian fluid	$10^2 \leq Ra \leq 10^4$; Obstacle position (B): $0.2H, 0.3H, 0.4H$	Triangular cavity with triangular obstacle.	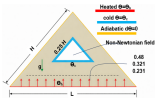
[42]	Mahmuda et al.	FEM	Al_2O_3–H_2O	$10^3 \leq Ra \leq 10^6$; $0 \leq Ha \leq 100$; $\phi = 0\%$–5%	Square cavity with a centrally placed heat-conducting triangular cylinder.	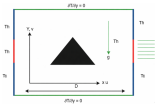
[43]	Maneengam et al.	GFEM	(Al_2O_3–Cu/H_2O)	$0 \leq Ha \leq 100$; $10^{-5} \leq Da \leq 10^{-2}$; $10^2 \leq Gr \leq 10^4$; $N = 2$–8	2D lid-driven porous cavity with obstacles.	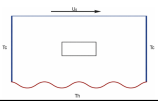

Note: FEM = Finite Element Method; LBM = Lattice Boltzmann Method; GFEM = Generalized Finite Element Method.

2.2 Cylinder and Circular Obstacles

Ghoben and Hussein [44] confirmed that the use of cylinders obstacles inside cavity enhances NC due to the increase in turbulent flow. double aligned cylinders have a negative effect on the Nu, while the best values of the Nu occur when double non-aligned cylinders. The cylindrical obstacles is enhancement and suppression of

HT within cavities. The HTR enhances with increasing heat source diameter, as a result of (Increased surface area for heat exchange) and that non-uniform heating gave best a result of (creating more effective gradients of temperature) [45]. The contradiction between the results of studies [44, 45] can be explained by several factors. First, the boundary conditions differ: study [44] employed uniform wall heating, while Jalili et al. [45] used non-uniform (sinusoidal) heating at the base of the cavity, which leads to different heat distribution patterns. Second, the geometric dimensionality varies, as Ghoben and Hussein [44] analyzed a three-dimensional cavity, whereas [45] focused on a two-dimensional one—significantly affecting flow behavior. Third, each study emphasized different characteristics: Ghoben and Hussein [44] examined the impact of obstacle alignment (aligned vs. non-aligned), while Jalili et al. [45] investigated the effect of obstacle number and size. Finally, the variation in heating methods and resulting flow patterns contributes to the differences in temperature fields and thermal performance, as reflected in the Nusselt number outcomes. Belmiloud et al. [46] investigated NC in a triangular cavity with inclined isothermal walls maintained at TC and a thermally insulated base. The cavity contains a cylindrical heat source at temperature TH and diameter D, placed within a nanofluid composed of H_2O and TiO_2. The study examines the effects of ($0.01 \leq \phi \leq 0.050$), ($10^3 \leq$ Ra $\leq 10^6$) and heat source position (h) on convective HT enhancement. Results indicate that thermal performance improves with increasing Ra, ϕ, and heat source diameter. These findings suggest significant potential for optimizing thermal management in systems employing nanofluid-filled triangular cavities with embedded heat sources.

Munir and Turabi [47] proved that the cold body in the middle of the cavity creates a large gradient of temperature between the cold obstacle, and the hot walls which enhances HT. The fluid is also forced to rotate around the obstacle, which enhances mixing and improves HT. It is also divided stream line and this creates thermal vortices that work to raise. Belhadj et al. [48] studied NC within a triangular cavity filled with (Ag-MgO-H_2O) under the influence of a magnetic field and featuring a rotating circular obstacle. The triangular cavity contains a porous quarter circle that is uniformly heated and is located at the right-angled corner. In this study, examined important parameters, including ($10^3 \leq$ Ra $\leq 10^6$), ($0 \leq$ Ha ≤ 80), ($10^{-5} \leq$ Da ≤ 0.15), rotational velocity (ω), and the circular radius (rob). The results indicated that HTR increases with the Ra and decreases with the increase of the Ha. The presence of a porous medium enhances HT, and increasing its thickness enhances HT. the variations in the obstacle's rotational velocity, size, and cavity geometry significantly influence transport of energy within the cavity.

Chabani et al. [49] studied the HT by a Cu-TiO_2/EG in a triangular, zigzag porous cavity containing different cylinders inside and exposed to an inclined magnetic field. The effect of several parameters was examined, including ($10^3 \leq$ Ra $\leq 10^6$), ($0 \leq$ Ha ≤ 100), ($0.02 \leq \phi \leq 0.08$), and the cylinder rotation speed (-400 $\leq$ w $\leq$ 4000). This study concluded that increasing all parameters will increase HTR except for the Ha, where the HTR decreases with Ha increase.

Bilal et al. [50] presented analysis of HT within a crown-shaped wavy cavity containing a centrally located heated circular obstacle, utilizing a (cu-cuo-Al_2O_3-H_2O). The effects of the obstacle's radius, (ϕ), Ra, and Ha under an inclined magnetic field were investigated. The results showed that increasing both the obstacle size and the (ϕ) significantly improved HTR, leading to an enhancement in the average Nu. In contrast, increasing the Ha suppressed fluid motion and reduced the efficiency of convective HT.

Aslam et al. [51] used FEM to analyze NC resulting from the temperature difference between the cavity walls and the internal obstacle. A H_2O was used to fill the three-dimensional, pyramid-shaped cavity with a hot, circular internal obstacle in the middle. This study found that the obstacle helped enhance HT, especially with non-uniform heating, as it contributed to the creation of strong thermal vortices, which enhanced the mixing between the hot and cold layers.

Turabi et al. [52] studied NC in a staggered Cavity containing a pair of compact circular cylinders. Cavity filled with (Cuo-Al_2O_3) with H_2O or ethylene glycol as the base fluid. This study found that each cylindrical obstacle acts as a barrier and creates strong vortex regions, which increases the mixing of the hybrid nanofluid and thus enhancement HT efficiency. The cylindrical obstacle increases turbulence and thus raises the Nu values.

Majeed et al. [53] investigated NC characteristics inside a hexagonal cavity containing a centrally placed heated circular obstacle. This numerical study using Casson fluid. The study contemplated the effects of the Ha, Aspect Ratio (AR), Casson number, Lewis number (Le), buoyancy ratio, and magnetic field inclination angle. The presence of the heated circular meaningfully improved local heat and mass transfer by generating strong vortical flows and thinning the thermal boundary layers. Increasing the obstacle size AR resulted in enhanced HTR, while the application of a magnetic field suppressed convection by magnetic damping. generally, the heated circular obstacle functioned as a crucial element in enhancing thermal performance in the hexagonal cavity.

Ali et al. [54] studied HT by using the FEM in a square cavity containing a solid heat-conducting circular obstacle, thermally conductive obstacle centered in the center of the cavity. A Casson fluid was used. This study proved that the circular obstacle generates strong vortices around it, which significantly changes the flow patterns. This in turn increases the turbulence in the flow and thus enhanced HTR.

Akhter et al. [55] investigated NC in a square cavity with a porous medium saturated with a hybrid nanofluid. The

effect of a hot cylindrical conductive barrier installed in the cavity center was studied. It was found that the cylindrical obstacle directly affects the flow distribution, creating vortices around the obstacle. This enhances thermal mixing and enhanced HT from the hot wall to the cold wall, thus increasing the Nu.

Shaker et al. [56] studied HT in a square cavity filled with H_2O containing five adiabatic cylindrical obstacles. This study found that the obstacles led to an increase in HTR and thus the Nu improved with increasing (10.4%, 12%, 16%, and 19%) respectively with the diameters of the obstacles (0.5, 1, 1.5, 2 cm). This study proved that with increasing the number of obstacles inside the cavity, an additional enhancement in HTR occurs.

Shirin [57] studied NC in a hexagonal cavity. The cavity contains air and a semicircular obstacle located in the cavity center. The results concluded that the semicircular obstacle led to a modification in the distribution of the streamlines, as multiple vortices were formed around the obstacle, thus stimulating convection currents, especially with the increase of the Ra Improved convection HT at high Ra, due to increased buoyancy force and increased formation of thin thermal boundary layers near the obstacle and hot walls.

Spizzichino et al. [58] analyzed the instability characteristics of a 3D NC flow inside a cold cubic cavity containing hot and cold horizontally aligned cylinders. Simulations at different cylinder distances and Ra revealed that the transition to unsteady flow occurs via the first Hopf bifurcation, preserving reflectional symmetries. The impact of cavity boundary proximity on flow instabilities was highlighted, clarifying how object orientation and spacing influence the spatiotemporal symmetries of slightly supercritical flows.

Shahzad et al. [59] analyzed double-diffusive NC within a triangular cavity containing an elliptic obstacle under the influence of a MF. Using the GFEM, the effects of important parameters such as Ha, Ra, Le, and magnetic field inclination were analyzed. Results indicated that the elliptic obstacle played an essential role in modifying flow patterns, intensifying vortical structures near the lower cavity, and improving the local heat and mass transfer. The obstacle, interacting with the MF, effectively controlled the thermal and concentration distributions. Table 2 shows a summary of previous studies related to the topic of the current research with regard to cylindrical and circular obstacles, in terms of reference, researchers, mathematical model, working fluid, study parameters, geometry, and physical model.

Table 2. Summary of the literature review relating to the current work: cylinder and circular obstacles

Ref.	Researchers	Math. Model	Working Fluid	Study Parameters	Geometry	Physical Model
[44]	Ghoben and Hussein	FEM	Al_2O_3–H_2O	$10^3 \leq Ra \leq 10^6$; $0.02 \leq \varphi \leq 0.05$	Triangular cavity with cylindrical obstacle.	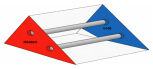
[45]	Jalili et al.	FEM	Al_2O_3–H_2O	$10^3 \leq Ra \leq 10^5$	Triangular cavity with cylindrical obstacle.	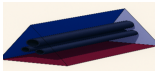
[46]	Belmiloud et al.	FEM	TiO_2–H_2O	$0.01 \leq \varphi \leq 0.050$; $10^3 \leq Ra \leq 10^6$	Triangular cavity with circular obstacle.	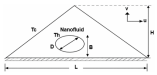
[47]	Munir and Turabi	FEM	Ag–MgO–H_2O	$0 \leq Ha \leq 50$; $10^2 \leq Ra \leq 10^6$; $0.01 \leq \varphi \leq 0.07$; $0° \leq \gamma \leq 90°$; $0 \leq N \leq 4$; $0.03 \leq \alpha \leq 0.1$	Triangular cavity with wavy base and a circular obstacle.	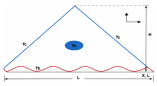
[48]	Belhadj et al.	FEM	Ag–MgO/H_2O	$10^3 \leq Ra \leq 10^6$; $2000 \leq \omega \leq +2000$	Triangular cavity with a circular obstacle.	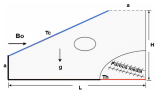
[49]	Chabani et al.	FEM	Cu–TiO_2/EG	$10^3 \leq Ra \leq 10^6$; $0 \leq Ha \leq 100$; $0.02 \leq \varphi \leq 0.08$; $-400 \leq \omega \leq 4000$	Triangular cavity with a sinuous chord and a circular obstacle.	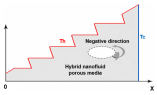
[50]	Bilal et al.	FEM	Cu–CuO–Al_2O_3/H_2O (Ternary hybrid nanofluid)	$10^3 \leq Ra \leq 10^5$; $0 \leq Ha \leq 100$; $\varphi = 0$–0.06; $R = 0.1$–0.2	Crown-shaped wavy cavity with a centrally heated circular obstacle.	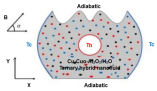

Ref.	Researchers	Math. Model	Working Fluid	Study Parameters	Geometry	Physical Model
[51]	Aslam et al.	FEM	Al_2O_3–H_2O	$10^4 \leq Ra \leq 10^6$; $0 \leq Ha \leq 100$; $\varphi = 0$–0.04; $0° \leq \gamma \leq 90°$	Pyramid-shaped cavity with internal hot circular obstacle.	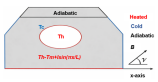
[52]	Turabi et al.	FEM	(Al_2O_3–Cu/ethylene glycol–H_2O)	$0 \leq Ha \leq 100$; $10^3 \leq Ra \leq 10^6$; $\phi = 0.01$–0.07; $0° \leq \gamma \leq 90°$	Staggered cavity with two embedded heated circular cylinders.	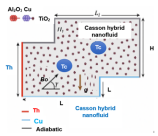
[53]	Majeed et al.	FEM	Casson fluid	$0 \leq Ha \leq 100$; $AR = 0.10$–0.20; $\beta = 1$–10; $Le = 1$–10; $0° \leq \gamma \leq 90°$	Hexagonal cavity with central heated circular obstacle.	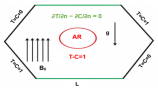
[54]	Ali et al.	FEM	Casson fluid	$Re = 1$–500; $\beta = 0.1$–5; $0 \leq Ha \leq 100$; $Pr = 20$	Square cavity with a central circular solid obstacle and double moving lids.	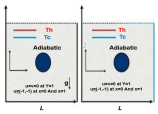
[55]	Akhter et al.	FEM	Cu–Al_2O_3/H_2O	$10^4 \leq Ra \leq 5 \times 10^6$; $0 \leq Ha \leq 100$; $\varphi = 0$–5%; $10^{-5} \leq Da \leq 10^{-2}$	Partially heated porous square cavity with central cylinder.	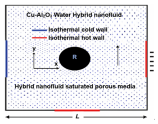
[56]	Shaker et al.	FVM	H_2O	$V = 0$–0.2 m/s; $r = 0.5$–2 cm; $Q = 400$–900 W	Rectangular lid-driven cavity with five adiabatic cylindrical obstacles.	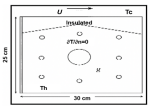
[57]	Shirin	FEM	Air	$10^3 \leq Ra \leq 10^6$; $Ha = 0$	Hexagonal cavity with a semi-circular cold obstacle at center.	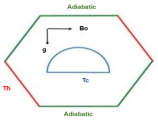
[58]	Spizzichino et al.	FVM	Air	$10^4 \leq Ra \leq 10^6$	Cubic cavity with two horizontal cylinders.	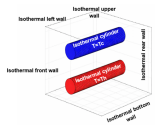
[59]	Shahzad et al	FEM	Viscous Newtonian fluid	$10^4 \leq Ra \leq 10^6$; $0 \leq Ha \leq 50$; $Le = 0.1$–10; $0° \leq \gamma \leq 90°$	Triangular cavity with central elliptic obstacle.	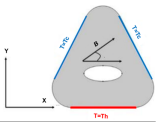

Note: FEM = Finite Element Method; FVM = Finite Volume Method.

2.3 Square and Rectangular Obstacles

Alsayegh [60] studied NC in a square cavity filled with a hybrid fluid. A hot rectangular obstacle is located in the center of the square cavity, connected to the bottom hot wall. the hot obstacle creates strong buoyancy-driven convection flows and strong thermal vortices are formed. This results in improved mixing and increased HT. However, increasing the obstacle size narrows the flow path, thus restricting the flow of the hot fluid and reducing the thermal efficiency.

Thilagavathi and Prasad [61] studied NC in a hexagonal cavity containing a cold square obstacle. The cavity is exposed to a magnetic field and filled with (Fe_3O_4 + TiO_2 + Cu-H_2O). The result of this study is that the presence of a cold obstacle enhances HT and increases the Nu. As the Ha increases, the Lorentz force is generated, weakening convection and shifting toward conduction-dominated HT.

Borahel et al. [62] investigated HT in a rectangular cavity filled with air, containing an isothermal square block placed at different location. The results showed that the block's location significantly affects the flow patterns within

the cavity. The study further confirmed that horizontally oriented cavities (low AR) produce higher Nu compared to vertically oriented cavities. Horizontal cavities (low AR) allow better flow circulation, thereby improving HT, whereas vertical cavities (high AR) cause flow confinement, which weakens the convective HT.

Santos et al. [63] A studied NC in a square open cavity containing 16 square, solid, thermally conductive obstacles. The obstacles are uniformly distributed within the cavity. The square, thermally conductive obstacles affect the flow in several ways: Directing internal flow through flow channels which alters the nature of the flow lines. Forming unyielded regions at high Bingham number. Influencing temperature distribution and creating a transition between natural and conductive convection modes. The presence of a centrally heated square obstacle in the lid-driven hexagonal cavity significantly modifies the flow and thermal fields. Higher Gr and Pr improve NC and overall HT, while higher Re suppress the buoyancy-driven flow leading to a conduction-dominated regime. Increasing the power-law index intensifies the velocity field and promotes stronger convective currents [64].

Ayaz [65] used LBM to numerically analyze a mixed convection in a square cavity with a square obstacle in the middle of the cavity. The cavity is filled with a viscous fluid. The results of this study show a comparison of the most important cases studied, where the case 1 was without an obstacle, the case 2 was a cold obstacle, and the case 3 was a hot obstacle. This study concluded that the hot obstacle gave the best results in increasing the HTR.

Bouaraour and Lebbi [66] studied of HT of a hybrid nanofluid filling a rectangular cavity with an (AR = 5) containing a rectangular hot obstacle. This study found that increasing (φ = 0.08) led to an improvement in the HTR by 9.8%. The obstacle also contributed to increasing the asymmetry of the flow, which improved the HT. The hot obstacle leads to an increase in the temperature gradient, and thus improved the overall thermal conductivity and thus increases the Nu by 4.5%.

Ali et al. [67] studied HT in a square cavity with a wavy bottom wall containing an inclined square obstacle, used FEM to investigated mixed convection of pure H_2O in cavity. This study concluded that the obstacle size affects the HTR. The incline of the obstacle improved the HT performance by enhancing the vortices generated around the obstacle and assisting in the free flow of the fluid. The presence of undulations within a certain number (3) also enhanced HT efficiency.

Sannad et al. [68] studied NC of 3D numerically using FVM with the (Boussinesq) approximation. 3D Cubical Cavity with Heated Partition. (Uniformly Heated Partition attached to the Left Wall). The results were summarized as follows: with high Ra, the thermal improvement was more evident, and the use of nanofluid increased the HT efficiency with increasing the (φ). The Heated Partition Induced Vortical Flow Structures and improved distribution of heat). The larger partition length resulted in improved NC due to the increased area of effective thermal.

Table 3 shows a summary of previous studies related to the topic of the current research with regard to square and rectangular obstacles, in terms of reference, researchers, mathematical model, working fluid, study parameters, geometry, and physical model.

Table 3. Summary of the literature review relating to the current work: square and rectangular obstacles

Ref.	Researchers	Math. Model	Working Fluid	Study Parameters	Geometry	Physical Model
[60]	Alsayegh	FVM	Cu–Al_2O_3–MWCNT/oil	$Ra = 5\times10^3$–5×10^4; $Ma = -10{,}000$ to $10{,}000$; φ = 0–0.06; h/w = 0.7–9	Square cavity with a hot baffle and free surface.	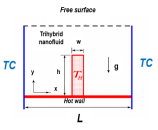
[61]	Thilagavathi and Prasad	FEM	Fe_3O_4–Cu–TiO_2 in H_2O	$Ra = 10^3$–10^5; Ha = 0–90; $Q = -5$–15; Pr = 29.86	Hexagonal cavity with a central square obstacle.	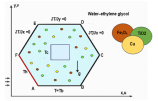
[62]	Borahel et al.	FVM	Air	Ri = 0.1, 1.0, 10; φ = 1/4, 1/8, 1/16, 1/32; AR = 0.10–3.0	Lid-driven cavity with a square isothermal block.	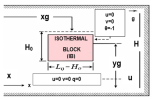
[63]	Santos et al.	FVM	Bingham viscoplastic fluid	$Ra = 10^5$–10^7; $Bn = 10^{-3}$–10; Pr = 500; κ = 10	Open square cavity with 16 uniformly distributed heated square blocks.	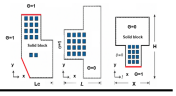

Ref.	Researchers	Math. Model	Working Fluid	Study Parameters	Geometry	Physical Model
[64]	Khan et al.	FEM	Power-law non-Newtonian fluid	$Re = 100$–400; $Pr = 1$–10; $Gr = 10^3$–10^6; $n = 0.5$–1.5	Hexagonal cavity with a central square obstacle.	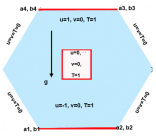
[65]	Ayaz	FVM	TiO_2–Cu/H_2O hybrid nanofluid	$Re = 100$; $Ri = 0.01$–1; $Gr = 10^2$–10^4; $\varphi = 0$–8%	Lid-driven cavity with a heated bottom obstacle.	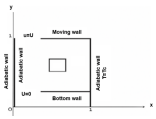
[66]	Bouaraour and Lebbi	FVM	TiO_2–Cu/H_2O hybrid nanofluid	$Re = 100$; $Ri = 0.01$–1; $Gr = 10^2$–10^4; $\varphi = 0$–8%	Lid-driven cavity with a heated bottom obstacle.	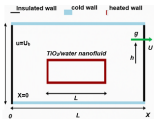
[67]	Ali et al.	FEM	H_2O	$Re = 10$–500; $Ri = 0.01$–10; $Ha = 0$–100; $Pr = 0.015$–10; $N = 1$–4; $D = 0.05$–0.2	Lid-driven square cavity with heated wavy bottom wall and tilted square obstacle.	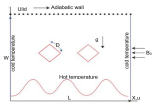
[68]	Sannad et al.	FVM	Cu–H_2O	$10^3 \leq Ra \leq 10^6$; $0 \leq \phi \leq 0.1$	A square cavity with rectangular obstacle.	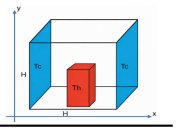

Note: FVM = Finite Volume Method; FEM = Finite Element Method.

2.4 Rhombic Obstacles

Nayak et al. [69] studied NC, and used the FEM for a nanofluid in a hexagonal cavity with a diamond-shaped cold obstacles inside cavity. This study relied on Ra, and Ha. The results showed that increasing the Ra from 10^5 to 10^6 improved the Nu by an increase of 76.16. The location of the rhomboidal obstacle affects the Nu When the obstacle is top of the cavity, the Nu increases by 6.3%. In the case 2, the obstacle is bottom of the cavity, the Nu decreases by 7.5%. (Positioning obstacles at the top enhanced NC due to higher density differences and stronger buoyancy flow). (Placing obstacles at the bottom weakened NC due to reduced buoyancy forces).

Rehman et al. [70] studied the NC of a Casson fluid in a square cavity with a porous medium. The cavity contains uniformly heated diamond-shaped obstacle. The results showed that increasing the Ra enhances the flow and increases HT. Increasing the Da also increases the permeability, thus reducing the flow resistance and accelerates the fluid velocity. The obstacle causes the formation of strong thermal vortices and a distinct pressure distribution inside the cavity, thus increasing Nu. Table 4 shows a summary of previous studies related to the topic of the current research with regard to specific obstacles, in terms of reference, researchers, mathematical model, working fluid, study parameters, geometry, and physical model.

Table 4. Summaryof the literatu rereview relatingtothe current work: rhombic obstacles

Ref.	Researchers	Math. Model	Working Fluid	Study Parameters	Geometry	Physical Model
[69]	Nayak et al.	FEM	Al_2O_3–H_2O	$Ra = 10^5$–10^6; $Ha = 0$–40; $\lambda = 0.3$–0.7; $\varphi = 2\%$	Hexagonal enclosure with cold diamond obstacles.	
[70]	Rehman et al.	FEM	Casson fluid	$Da = 10^{-5}$–10^{-3}; $Pr = 20$; $\beta_p = 0.1$	Square porous cavity with diamond obstacle.	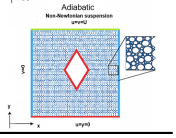

Note: FEM = Finite Element Method.

3 The Governing Equations

Numerical solutions are an essential tool for studying (3D-NC) within cavities of various geometric shapes. A set of governing equations is used according to the nature of the study, whether in steady-state or unsteady-state conditions. These equations (1–5), which are used to describe fluid motion and HT within it. In this research, the unsteady form of these equations will be shown for both conventional and nanofluid respectively [71].

3.1 The Classical Fluids Governing Equations

The continuity equation [72]:

$$\frac{\partial u}{\partial x}+\frac{\partial v}{\partial y}+\frac{\partial w}{\partial z}=0 \tag{1}$$

The momentum equation [72]
x-direction:

$$\frac{\partial u}{\partial t}+u\frac{\partial u}{\partial x}+v\frac{\partial u}{\partial y}+w\frac{\partial u}{\partial z}=-\frac{1}{\rho}\frac{\partial P}{\partial x}+v\left(\frac{\partial^2 u}{\partial x^2}+\frac{\partial^2 u}{\partial y^2}+\frac{\partial^2 u}{\partial z^2}\right) \tag{2}$$

y-direction [72]:

$$\frac{\partial v}{\partial t}+u\frac{\partial v}{\partial x}+v\frac{\partial v}{\partial y}+w\frac{\partial v}{\partial z}=-\frac{1}{\rho}\frac{\partial P}{\partial y}+v\left(\frac{\partial^2 v}{\partial x^2}+\frac{\partial^2 v}{\partial y^2}+\frac{\partial^2 v}{\partial z^2}\right) \tag{3}$$

z-direction [72]:

$$\frac{\partial w}{\partial t}+u\frac{\partial w}{\partial x}+v\frac{\partial w}{\partial y}+w\frac{\partial w}{\partial z}=-\frac{1}{\rho}\frac{\partial P}{\partial z}+v\left(\frac{\partial^2 w}{\partial x^2}+\frac{\partial^2 w}{\partial y^2}+\frac{\partial^2 w}{\partial z^2}\right)+\rho g\beta\left(T-T_c\right) \tag{4}$$

The energy equation [72]:

$$\frac{\partial T}{\partial t}+u\frac{\partial T}{\partial x}+v\frac{\partial T}{\partial y}+w\frac{\partial T}{\partial z}=\alpha\left(\frac{\partial^2 T}{\partial x^2}+\frac{\partial^2 T}{\partial y^2}+\frac{\partial^2 T}{\partial z^2}\right) \tag{5}$$

3.2 The Nanofluids Governing Equations

In the case of nanofluids, the governing equations are modified to account for the presence of solid nanoparticles, which alter the fluid's effective thermophysical properties for instance thermal conductivity, viscosity, and density [73]:

$$\frac{\partial u}{\partial x}+\frac{\partial v}{\partial y}+\frac{\partial w}{\partial z}=0 \tag{6}$$

The momentum equation [73]
x-direction:

$$\rho_{nf}\left(\frac{\partial u}{\partial t}+u\frac{\partial u}{\partial x}+v\frac{\partial u}{\partial y}+w\frac{\partial u}{\partial z}\right)=-\frac{\partial P}{\partial x}+\mu_{nf}\left(\frac{\partial^2 u}{\partial x^2}+\frac{\partial^2 u}{\partial y^2}+\frac{\partial^2 u}{\partial z^2}\right) \tag{7}$$

y-direction:

$$\rho_{nf}\left(\frac{\partial v}{\partial t}+u\frac{\partial v}{\partial x}+v\frac{\partial v}{\partial y}+w\frac{\partial v}{\partial z}\right)=-\frac{\partial P}{\partial y}+\mu_{nf}\left(\frac{\partial^2 v}{\partial x^2}+\frac{\partial^2 v}{\partial y^2}+\frac{\partial^2 v}{\partial z^2}\right)-\rho_{nf}g \tag{8}$$

z-direction:

$$\rho_{nf}\left(\frac{\partial w}{\partial t}+u\frac{\partial w}{\partial x}+v\frac{\partial w}{\partial y}+w\frac{\partial w}{\partial z}\right)=-\frac{\partial P}{\partial z}+\mu_{nf}\left(\frac{\partial^2 w}{\partial x^2}+\frac{\partial^2 w}{\partial y^2}+\frac{\partial^2 w}{\partial z^2}\right) \tag{9}$$

The energy equation:

$$\frac{\partial T}{\partial t}+u\frac{\partial T}{\partial x}+v\frac{\partial T}{\partial y}+w\frac{\partial T}{\partial z}=\alpha_{nf}\left(\frac{\partial^2 T}{\partial x^2}+\frac{\partial^2 T}{\partial y^2}+\frac{\partial^2 T}{\partial z^2}\right) \tag{10}$$

where, ρ_{nf}, μ_{nf}, α_{nf} are given by [74]:

$$\rho_{nf}=(1-\varphi)\rho_f+\varphi\rho_s \tag{11}$$

$$\mu_{nf}=\frac{\mu_f}{(1-\varphi)^{2.5}} \tag{12}$$

$$\alpha_{nf}=\frac{k_{nf}}{(\rho C_p)_{nf}} \tag{13}$$

$$(\rho C_p)_{nf}=(1-\varphi)\,(\rho C_p)_f+\varphi\,(\rho C_p)_s \tag{14}$$

Maxwell gave the equation below [75]:

$$\frac{k_{nf}}{k_f}=1+\frac{3\left(\frac{k_s}{k_f}-1\right)\varphi}{\left(\frac{k_s}{k_f}+2\right)-\left(\frac{k_s}{k_f}-1\right)\varphi} \tag{15}$$

Hamilton and Crosser [76] developed the Eq. (15) and it became

$$\frac{k_{nf}}{k_f}=\frac{k_s+(n-1)k_f-(n-1)\varphi\,(k_f-k_s)}{k_s+(n-1)k_f+\varphi\,(k_f-k_s)} \tag{16}$$

The parameter n represents the shape factor, typically taken as 6 for cylindrical particles and 3 for spherical ones. For spherical nanoparticles, an approximation can be made using the Maxwell-Garnett model [75], expressed as:

$$\frac{k_{nf}}{k_f}=\frac{k_s+2k_f-2\varphi\,(k_f-k_s)}{k_s+2k_f+\varphi\,(k_f-k_s)} \tag{17}$$

Several advanced models have been developed to account for nanoparticle interactions by incorporating higher-order terms, such as those proposed by Jeffrey [77].

$$\frac{k_{nf}}{k_f}=1+3\beta\varphi+\left(3\beta^2+\frac{3\beta^2}{4}+\frac{9\beta^3}{16}\frac{\alpha+2}{2\alpha+3}+\cdots\right)\varphi^2 \tag{18}$$

where,

$$\beta=\frac{\left(\frac{k_s}{k_f}-1\right)}{\left(\frac{k_s}{k_f}+2\right)} \tag{19}$$

And the model of Arul Raja [78] as:

$$\frac{k_{nf}}{k_f} = 1 + \frac{3\left(\frac{k_s}{k_f} - 1\right)}{\left(\frac{k_s}{k_f} + 2\right) - \left(\frac{k_s}{k_f} - 1\right)\varphi}\left[\varphi + f\left(\frac{k_s}{k_f}\right)\varphi^2 + O\left(\varphi^3\right)\right] \tag{20}$$

where, $f(8) = 0.5$ and $f(10) = 2.5$.

The equations below are the governing non-dimensional equations.

$$\mathrm{X} = \frac{x}{H}\mathrm{Y} = \frac{y}{H}Z = \frac{z}{H}U = \frac{uH}{\alpha_- f}V = \frac{vH}{\alpha_- f}W = \frac{wH}{\alpha_- f}$$

$$P = \frac{pH^2}{\rho_f \alpha_f^2}\theta = \frac{T - T_{ref}}{T_H - T_C}T_{ref} = \frac{T_C + T_H}{2}Ra = \frac{g\beta_f H^3\left(T_H - T_C\right)}{\vartheta_f \alpha_f}Pr = \frac{\vartheta_f}{\alpha_f}$$

The continuity equation:

$$\frac{\partial U}{\partial X} + \frac{\partial V}{\partial Y} + \frac{\partial W}{\partial Z} = 0 \tag{21}$$

The momentum equations
x-direction:

$$U\frac{\partial U}{\partial X} + v\frac{\partial U}{\partial Y} + w\frac{\partial U}{\partial Z} = -\frac{\partial U}{\partial X} + \mathrm{Pr}\left(\frac{\partial^2 U}{\partial X^2} + \frac{\partial^2 U}{\partial Y^2} + \frac{\partial^2 U}{\partial Z^2}\right) \tag{22}$$

y-direction:

$$U\frac{\partial V}{\partial X} + v\frac{\partial V}{\partial Y} + w\frac{\partial V}{\partial Z} = -\frac{\partial P}{\partial Y} + \mathrm{Pr}\left(\frac{\partial^2 V}{\partial X^2} + \frac{\partial^2 V}{\partial Y^2} + \frac{\partial^2 V}{\partial Z^2}\right) + \mathrm{RaPr}\,\theta \tag{23}$$

The energy equation:

$$u\frac{\partial \theta}{\partial x} + v\frac{\partial \theta}{\partial y} + w\frac{\partial \theta}{\partial z} = \left(\frac{\partial^2 \theta}{\partial X^2} + \frac{\partial^2 \theta}{\partial Y^2} + \frac{\partial^2 \theta}{\partial Z^2}\right) \tag{24}$$

The governing equations above are presented in a general form. In specific numerical studies, boundary conditions (such as isothermal or adiabatic walls) are defined based on the problem setup and objectives.

4 Conclusions

• Using a triangular obstacle increased the Nusselt number by 76.16% at Ra = 10^6, highlighting the significant impact of obstacle shape on heat transfer efficiency.

• Non-aligned cylindrical obstacles showed better thermal performance than aligned arrangements.

• Cylindrical obstacles outperformed square ones by 15%–20% in enhancing thermal performance under the same flow conditions.

• Complex obstacle shapes, such as “T” and “U”, can be utilized in the design of heat sinks for electronic devices.

• These shapes help improve temperature distribution and enhance heat exchange zones within thermal systems.

• Most of the studies conducted are numerical studies and there is a clear lack of experimental studies.

• There is a focus on two-dimensional numerical studies and a lack of three-dimensional numerical studies.

• The shapes of Obstacles were limited to classical shapes (square, triangular, circle, etc.) without touching upon complex shapes such as literal shapes (U, L, T, Y, M, . . . , etc.).

• The boundary conditions of the obstacles vary. Obstacles may be hot, cold, or adiabatic. This directly affects the HT performance, and Nu values.

• Hybrid nanofluids gave better results than other conventional fluids and mono nanofluids.

• Internal obstacles (cold or hot) play a vital role in increasing HTR by enhancing the temperature gradient and enhancing vortices.

• Obstacles are considered one of the most important means of controlling HTR, as their location within cavities plays a prominent role in changing the velocity and temperature distribution within the cavity, which enhancing or obstructs convection depending on the obstacle position.

• The Nu is clearly affected by the shape of the obstacle (square, rectangle, circle, etc.). Different shapes lead to different flow and vortex patterns, and thus change the thermal performance.

• In natural convection, an obstacle can either impedes or improve the buoyancy force. In mixed convection, or magnetic field-induced (MHD), the obstacle effect becomes more complex.

• Most obstructions enhance thermal performance but may increase entropy generation (this is important for analyzing overall thermal efficiency).

• Although the majority of studies reviewed are numerical, there is a critical need for experimental validation to support and verify these findings.

• Future research should focus on experimental implementations, grid independence tests, and benchmarking against existing experimental data to enhance reliability and practical applicability.

Data Availability

The data used to support the findings of this study are available from the corresponding author upon request.

Conflicts of Interest

The authors declare that they have no conflicts of interest.

References

[1] C. N. Mithun, M. J. Hasan, A. K. Azad, R. Hossain, and M. M. Rahman, "Double-diffusive unsteady flow in a roof-based air ventilation system with variable Prandtl number," *Arab. J. Sci. Eng.*, vol. 48, pp. 12 125–12 140, 2022. https://doi.org/10.1007/s13369-022-07453-6

[2] S. Saravanan and C. Sivaraj, "Combined natural convection and thermal radiation in a square cavity with a nonuniformly heated plate," *Comput. Fluids*, vol. 117, pp. 125–138, 2015. https://doi.org/10.1016/j.compfluid.2015.05.005

[3] U. Rashid, D. Lu, and Q. Iqbal, "Nanoparticles impacts on natural convection nanofluid flow and heat transfer inside a square cavity with fixed a circular obstacle," *Case Stud. Therm. Eng.*, vol. 44, p. 102829, 2023. https://doi.org/10.1016/j.csite.2023.102829

[4] I. Hashim, A. Alsabery, M. Sheremet, and A. Chamkha, "Numerical investigation of natural convection of Al_2O_3-H_2O nanofluid in a wavy cavity with conductive inner block using Buongiorno's two-phase model," *Adv. Powder Technol.*, vol. 30, no. 2, pp. 399–414, 2019. https://doi.org/10.1016/j.apt.2018.11.017

[5] S. Nasir, A. S. Berrouk, A. Aamir, and T. Gul, "Significance of chemical reactions and entropy on Darcy–Forchheimer flow of H_2O and $C_2H_6O_2$ convening magnetized nanoparticles," *Int. J. Thermofluids*, vol. 17, p. 100265, 2023. https://doi.org/10.1016/j.ijft.2022.100265

[6] M. Sadeghi, A. S. Dogonchi, M. Ghodrat, J. A. Chamkha, H. Alhumade, and N. Karimi, "Natural convection of CuO-H_2O nanofluid in a conventional oil/H_2O separator cavity: Application to combined-cycle power plants," *J. Taiwan Inst. Chem. Eng.*, vol. 124, pp. 307–319, 2021. https://doi.org/10.1016/j.jtice.2021.03.031

[7] M. Sheikhpour, M. Arabi, A. Kasaeian, A. R. Rabei, and Z. Taherian, "Role of nanofluids in drug delivery and biomedical technology: Methods and applications," *Nanotechnol. Sci. Appl.*, vol. 13, pp. 47–59, 2020. https://doi.org/10.2147/NSA.S260374

[8] F. Abbas, H. M. Ali, T. R. Shah, H. Babar, M. M. Janjua, U. Sajjad, and M. Amer, "Nanofluid: Potential evaluation in automotive radiator," *J. Mol. Liq.*, vol. 297, p. 112014, 2020. https://doi.org/10.1016/j.molliq.2019.112014

[9] Z. Li, A. K. Hussein, O. Younis, S. Rostami, and W. He, "Effect of alumina nano-powder on the natural convection of H_2O under the influence of a magnetic field in a cavity and optimization using RMS: Using empirical correlations for the thermal conductivity and a sensitivity analysis," *Int. Commun. Heat Mass Transf.*, vol. 112, p. 104497, 2020. https://doi.org/10.1016/j.icheatmasstransfer.2020.104497

[10] M. B. Cherif, A. Abderrahmane, A. M. Saeed, N. Qasem, O. Younis, R. Marzouki, J. D. Chung, and N. A. Shah, "Hydrothermal and entropy investigation of nanofluid mixed convection in triangular cavity with wavy boundary heated from below and rotating cylinders," *Nanomaterials*, vol. 12, no. 9, p. 1469, 2022. https://doi.org/10.3390/nano12091469

[11] Z. H. Khan, W. A. Khan, M. Qasim, S. O. Alharbi, M. Hamid, and M. Du, "Hybrid nanofluid flow around a triangular-shaped obstacle inside a split lid-driven trapezoidal cavity," *Eur. Phys. J. Spec. Top.*, vol. 231, no. 13, pp. 2749–2759, 2022. https://doi.org/10.1140/epjs/s11734-022-00607-5

[12] M. Abed, A. Abderrahmane, O. Younis, R. Marzouki, and A. Alazzam, "Numerical simulations of magnetohydrodynamics natural convection and entropy production in a porous annulus bounded by wavy cylinder and Koch snowflake loaded with Cu–H_2O nanofluid," *Micromachines*, vol. 13, no. 2, p. 182, 2022. https://doi.org/10.3390/mi13020182

[13] A. D. Abdulsahib, A. S. Hashim, K. Al-Farhany, A. Abdulkadhim, and F. Mebarek-Oudina, "Natural convection investigation under influence of internal bodies within a nanofluid-filled square cavity," *Eur. Phys. J. Spec. Top.*, vol. 231, no. 13, pp. 2605–2621, 2022. https://doi.org/10.1140/epjs/s11734-022-00584-9

[14] M. A. Adriana, "Challenges in hybrid nanofluids behavior in turbulent flow: Recent research and numerical comparison," *Renew. Sustain. Energy Rev.*, vol. 71, pp. 426–434, 2017. https://doi.org/10.1016/j.rser.2016.12.072

[15] R. Turcu, A. L. Darabont, A. Nan, N. Aldea, D. Macovei, D. Bica, and L. Vekas, "New polypyrrole-multiwall carbon nanotubes hybrid materials," *J. Optoelectron. Adv. Mater.*, vol. 8, no. 2, pp. 643–647, 2006. https://old.joam.inoe.ro/arhiva/pdf8_2/Turcu.pdf

[16] G. Huminic and A. Huminic, "Hybrid nanofluids for heat transfer applications–a state-of-the-art review," *Int. J. Heat Mass Transf.*, vol. 125, pp. 82–103, 2018. https://doi.org/10.1016/j.ijheatmasstransfer.2018.04.059

[17] S. Nasir, A. S. Berrouk, and A. Aamir, "Exploring nanoparticle dynamics in binary chemical reactions within magnetized porous media: A computational analysis," *Sci. Rep.*, vol. 14, no. 1, p. 25505, 2024. https://doi.org/10.1038/s41598-024-76757-4

[18] A. J. Chamkha, I. V. Miroshnichenko, and M. A. Sheremet, "Numerical analysis of unsteady conjugate natural convection of hybrid H_2O-based nanofluid in a semicircular cavity," *J. Therm. Sci. Eng. Appl.*, vol. 9, no. 4, p. 041004, 2017. https://doi.org/10.1115/1.4036203

[19] S. Nasir and A. S. Berrouk, "Comparative study of computational frameworks for magnetite and carbon nanotube-based nanofluids in enclosure," *J. Therm. Anal. Calorim.*, vol. 149, no. 5, pp. 2403–2423, 2024. https://doi.org/10.1007/s10973-023-12811-z

[20] L. Yang and B. Farouk, "Mixed convection around a heated rotating horizontal square cylinder in a circular enclosure," *Numer. Heat Transf. A Appl.*, vol. 28, no. 1, pp. 1–18, 1995. https://doi.org/10.1080/10407789508913729

[21] F. Moukalled and S. Acharya, "Natural convection in the annulus between concentric horizontal circular and square cylinders," *J. Thermophys. Heat Transf.*, vol. 10, no. 3, pp. 524–531, 1996. https://doi.org/10.2514/3.820

[22] S. Nasir, S. Sirisubtawee, P. Juntharee, A. S. Berrouk, S. Mukhtar, and T. Gul, "Heat transport study of ternary hybrid nanofluid flow under magnetic dipole together with nonlinear thermal radiation," *Appl. Nanosci.*, vol. 12, no. 9, pp. 2777–2788, 2022. https://doi.org/10.1007/s13204-022-02583-7

[23] S. Dutta, N. Goswami, A. K. Biswas, and S. Pati, "Numerical investigation of magnetohydrodynamic natural convection heat transfer and entropy generation in a rhombic enclosure filled with Cu-H_2O nanofluid," *Int. J. Heat Mass Transf.*, vol. 136, pp. 777–798, 2019. https://doi.org/10.1016/j.ijheatmasstransfer.2019.03.024

[24] S. Nasir, A. S. Berrouk, and T. Gul, "Analysis of chemical reactive nanofluid flow on stretching surface using numerical soft computing approach for thermal enhancement," *Eng. Appl. Comput. Fluid Mech.*, vol. 18, no. 1, p. 2340609, 2024. https://doi.org/10.1080/19942060.2024.2340609

[25] K. S. Saha, "Magnetohydrodynamic buoyancy driven Al_2O_3-H_2O nanofluid flow in a differentially heated trapezoidal enclosure with a cylindrical barrier," *Int. Commun. Heat Mass Transf.*, vol. 114, p. 104593, 2020. https://doi.org/10.1016/j.icheatmasstransfer.2020.104593

[26] B. P. Geridonmez and H. F. Oztop, "MHD natural convection in a cavity in the presence of cross partial magnetic fields and Al_2O_3-H_2O nanofluid," *Comput. Math. Appl.*, vol. 80, no. 12, pp. 2796–2810, 2020. https://doi.org/10.1016/j.camwa.2020.10.003

[27] M. Alsabery, E. Gedik, A. J. Chamkha, and I. Hashim, "Impacts of heated rotating inner cylinder and two-phase nanofluid model on entropy generation and mixed convection in a square cavity," *Heat Mass Transf.*, vol. 56, no. 1, pp. 321–338, 2020. https://doi.org/10.1007/s00231-019-02698-8

[28] P. Sreedevi and P. S. Reddy, "Effect of magnetic field and thermal radiation on natural convection in a square cavity filled with TiO_2 nanoparticles using Tiwari-Das model," *Alex. Eng. J.*, vol. 61, no. 2, pp. 1529–1541, 2022. https://doi.org/10.1016/j.aej.2021.06.055

[29] S. Saravanan and C. Sivaraj, "Combined thermal radiation and natural convection in a cavity containing a discrete heater: Effects of nature of heating and heater aspect ratio," *Int. J. Heat Fluid Flow*, vol. 66, pp. 70–82, 2017. https://doi.org/10.1016/j.ijheatfluidflow.2017.05.004

[30] A. Rahimi, A. Kasaeipoor, and E. H. Malekshah, "Natural convection analysis by entropy generation and heatline visualization using lattice Boltzmann method in nanofluid filled cavity included with internal heaters-empirical thermo-physical properties," *Int. J. Mech. Sci.*, vol. 133, pp. 199–216, 2017. https://doi.org/10.1016/j.ijmecsci.2017.08.044

[31] M. J. Uddin, S. K. Rasel, M. M. Rahman, and K. Vajravelu, "Natural convective heat transfer in a nanofluid-filled square vessel having a wavy upper surface in the presence of a magnetic field," *Therm. Sci. Eng. Prog.*, vol. 19, p. 100660, 2020. https://doi.org/10.1016/j.tsep.2020.100660

[32] M. A. Sheremet, I. Pop, and A. Shenoy, "Unsteady free convection in a porous open wavy cavity filled with

a nanofluid using Buongiorno's mathematical model," *Int. Commun. Heat Mass Transf.*, vol. 67, pp. 66–72, 2015. https://doi.org/10.1016/j.icheatmasstransfer.2015.07.007

[33] M. A. Ismael, E. Abu-Nada, and A. J. Chamkha, "Mixed convection in a square cavity filled with CuO-H_2O nanofluid heated by corner heater," *Int. J. Mech. Sci.*, vol. 133, pp. 42–50, 2017. https://doi.org/10.1016/j.ijmecsci.2017.08.029

[34] K. Kalidasan and P. R. Kanna, "Natural convection on an open square cavity containing diagonally placed heaters and adiabatic square block and filled with hybrid nanofluid of nanodiamond-cobalt oxide/water," *Int. Commun. Heat Mass Transf.*, vol. 81, pp. 64–71, 2017. https://doi.org/10.1016/j.icheatmasstransfer.2016.12.005

[35] R. Mohebbi and M. M. Rashidi, "Numerical simulation of natural convection heat transfer of a nanofluid in an L-shaped enclosure with a heating obstacle," *J. Taiwan Inst. Chem. Eng.*, vol. 72, pp. 70–84, 2017. https://doi.org/10.1016/j.jtice.2017.01.006

[36] A. E. M. Bouchoucha, R. Bessaïh, H. F. Oztop, K. Al-Salem, and F. Bayrak, "Natural convection and entropy generation in a nanofluid filled cavity with thick bottom wall: Effects of non-isothermal heating," *Int. J. Mech. Sci.*, vol. 126, pp. 95–105, 2017. https://doi.org/10.1016/j.ijmecsci.2017.03.025

[37] B. Al-Muhjaa and K. Al-Farhany, "Numerical investigation of the effect of baffle inclination angle on nanofluid natural convection heat transfer in a square enclosure," *Al-Qadisiyah J. Eng. Sci.*, vol. 12, pp. 61–71, 2019. https://doi.org/10.30772/qjes.v12i2.589

[38] T. Armaghani, A. Kasaeipoor, N. Alavi, and M. M. Rashidi, "Numerical investigation of H_2O-alumina nanofluid natural convection heat transfer and entropy generation in a baffled L-shaped cavity," *J. Mol. Liq.*, vol. 223, pp. 243–251, 2016. https://doi.org/10.1016/j.molliq.2016.07.103

[39] D. Chatterjee, N. K. Manna, and N. Biswas, "Thermo-magnetic convection of nanofluid in a triangular cavity with a heated inverted triangular object," *Mater. Today Proc.*, vol. 52, pp. 427–433, 2022. https://doi.org/10.1016/j.matpr.2021.11.474

[40] H. Roshani, B. Jalili, A. Mirzaei, P. Jalili, and D. D. Ganji, "The effect of buoyancy force on natural convection heat transfer of nanofluid flow in triangular cavity with different barriers," *Heliyon*, vol. 10, p. e35690, 2024. https://doi.org/10.1016/j.heliyon.2024.e35690

[41] D. T. Yaseen, A. J. Majeed, A. Al-Mukhtar, E. Gomaa, and A. A. Nassar, "Controlling convective heat transfer of shear thinning fluid in a triangular enclosure with different obstacle positions," *Case Stud. Therm. Eng.*, vol. 61, p. 105003, 2024. https://doi.org/10.1016/j.csite.2024.105003

[42] S. Mahmuda and M. M. Ali, "MHD free convection flow of nanofluids inside a flush mounted heated square cavity containing a heat conducting triangular cylinder," 2024, Mawlana Bhashani Science and Technology University. https://doi.org/10.21203/rs.3.rs-4840716/v1

[43] A. Maneengam, H. Laidoudi, A. Abderrahmane, G. Rasool, K. Guedri, W. Weera, and B. Bouallegue, "Entropy generation in 2D lid-driven porous container with the presence of obstacles of different shapes and under the influences of buoyancy and Lorentz forces," *Nanomaterials*, vol. 12, no. 13, p. 2206, 2022. https://doi.org/10.3390/nano12132206

[44] Z. K. Ghoben and A. K. Hussein, "The natural convection inside a 3D triangular cross-section cavity filled with nanofluid and included cylinder with different arrangements," *Diagnostyka*, vol. 23, no. 2, p. 2022205, 2022. https://doi.org/10.29354/diag/149734

[45] B. Jalili, H. Roshani, P. Jalili, and D. D. Ganji, "Numerical study of Newtonian fluid flow characteristics in triangle enclosure considering various obstacle geometries," *Int. J. Thermofluids*, vol. 20, p. 100515, 2023. https://doi.org/10.1016/j.ijft.2023.100515

[46] M. A. Belmiloud, S. Mekroussi, B. Mebarek, H. M. Meghazi, and M. S. M. Saleh, "Thermal source effect on the natural convection of a nanofluid within a triangular cavity," *Appl. Eng. Lett.*, vol. 9, no. 2, pp. 94–104, 2024. https://doi.org/10.46793/aeletters.2024.9.2.4

[47] S. Munir and Y. U. U. B. Turabi, "Impact of heated wavy wall and hybrid nanofluid on natural convection in a triangular enclosure with embedded cold cylinder under inclined magnetic field," *Arab. J. Sci. Eng.*, vol. 50, pp. 4007–4020, 2024. https://doi.org/10.1007/s13369-024-09450-3

[48] M. A. Belhadj, F. Redouane, L. Mourad, W. Jamshed, M. R. Eid, and W. Al-Kouz, "Magnetohydrodynamics natural convection of a triangular cavity involving Ag-MgO/H_2O hybrid nanofluid and provided with rotating circular barrier and a quarter circular porous medium at its right-angled corner," *Arab. J. Sci. Eng.*, vol. 46, no. 12, pp. 12 573–12 597, 2021. https://doi.org/10.1007/s13369-021-06015-6

[49] I. Chabani, F. Mebarek-Oudina, and A. A. I. Ismail, "MHD flow of a hybrid nano-fluid in a triangular enclosure with zigzags and an elliptic obstacle," *Micromachines*, vol. 13, no. 2, p. 224, 2022. https://doi.org/10.3390/mi13020224

[50] S. Bilal, I. A. Shah, A. S. Alqahtani, and M. Y. Malik, "Significance of aspect ratio of internal heating element in optimizing thermal production of H_2O with ternary nano composition in crown chamber," *Case Stud. Therm.*

Eng., vol. 68, p. 105882, 2025. https://doi.org/10.1016/j.csite.2025.105882

[51] M. A. Aslam, L. Yang, X. Chen, H. Shahzad, and K. Zhang, "Hydro-thermal analysis of magnetize nanofluid inside pyramid shape enclosure under the effect of non-uniform heating," *Case Stud. Therm. Eng.*, vol. 70, p. 106105, 2025. https://doi.org/10.1016/j.csite.2025.106105

[52] Y. U. U. Turabi, S. Munir, and R. Nawaz, "Entropy generation and magnetohydrodynamic influences on hybrid nanofluid convection in a staggered cavity," *Int. J. Thermofluids*, vol. 27, p. 101204, 2025. https://doi.org/10.1016/j.ijft.2025.101204

[53] A. H. Majeed, M. J. Hasan, H. Waqas, D. Liu, R. Alroobaea, and T. Muhammad, "Impact of Hartmann number and aspect ratio on the heat and mass transfer characteristics in a hexagonal enclosure with a heated circular obstacle inside," *Ain Shams Eng. J.*, vol. 16, no. 4, p. 103330, 2025. https://doi.org/10.1016/j.asej.2025.103330

[54] M. M. Ali, R. Akhter, and M. A. Alim, "Performance of flow and heat transfer analysis of mixed convection in Casson fluid filled lid-driven cavity including solid obstacle with magnetic impact," *SN Appl. Sci.*, vol. 3, p. 250, 2021. https://doi.org/10.1007/s42452-021-04243-x

[55] R. Akhter, M. M. Ali, and M. A. Alim, "Entropy generation due to hydromagnetic buoyancy-driven hybrid-nanofluid flow in partially heated porous cavity containing heat conductive obstacle," *Alex. Eng. J.*, vol. 62, pp. 17–45, 2023. https://doi.org/10.1016/j.aej.2022.07.005

[56] A. M. Shaker, N. J. Yasin, H. A. Ameen, and A. S. Abedalh, "Obstacle arrangements effect on the mixed convection in an enclosure with movable top surface," *J. Appl. Res. Technol.*, vol. 22, pp. 806–815, 2024. https://doi.org/10.22201/icat.24486736e.2024.22.6.2576

[57] G. H. Shirin, "Computational investigation of natural convection on a hexagonal cavity with a semi-circular cooler obstacle," *J. Eden Mohila Coll.*, vol. 4, pp. 75–85, 2024. https://emc.edu.bd/wp-content/uploads/2025/03/Gazi-Homayra-Shirin.pdf

[58] A. Spizzichino, E. Zemach, and Y. Feldman, "Oscillatory instability of a 3D natural convection flow around a tandem of cold and hot vertically aligned cylinders placed inside a cold cubic enclosure," *Int. J. Heat Mass Transf.*, vol. 141, pp. 327–345, 2019. https://doi.org/10.1016/j.ijheatmasstransfer.2019.06.050

[59] H. Shahzad, A. Ghaffari, G. Rasool, Q. Ma, and Y. Li, "Exploring MHD-generated flow in a triangular cavity having an elliptic obstruction: implications for industrial applications," *Sci. Iran.*, vol. 32, 2025. https://doi.org/10.24200/sci.2025.62407.7824

[60] R. Alsayegh, "Numerical investigation of trihybrid nanofluid heat transfer in a cavity with a hot baffle," *Case Stud. Therm. Eng.*, vol. 65, p. 105584, 2025. https://doi.org/10.1016/j.csite.2024.105584

[61] A. Thilagavathi and V. R. Prasad, "Thermal heat transfer enhancement analysis of magnetic ternary hybrid nanofluid in a hexagonal cavity with square obstacle," *J. Appl. Comput. Mech.*, vol. 11, no. 1, pp. 239–252, 2025. https://doi.org/10.22055/jacm.2024.46544.4548

[62] R. D. S. Borahel, F. S. F. Zinani, L. A. Isoldi, E. D. Dos Santos, and L. A. O. Rocha, "Analysis of the design of cavities with isothermal blocks under mixed convection," *J. Appl. Comput. Mech.*, vol. 11, no. 2, pp. 541–556, 2025. https://doi.org/10.22055/jacm.2024.47208.4676

[63] P. R. Santos, A. T. Franco, and S. L. Junqueira, "Numerical investigation of viscoplastic fluids on natural convection in open cavities with solid obstacles," *Heliyon*, vol. 10, no. 4, p. e26243, 2024. https://doi.org/10.1016/j.heliyon.2024.e26243

[64] Y. Khan, A. H. Majeed, H. Shahzad, F. J. Awan, K. Iqbal, M. Ajmal, and N. Faraz, "Numerical computations of non-Newtonian fluid flow in hexagonal cavity with a square obstacle: A hybrid mesh–based study," *Front. Phys.*, vol. 10, p. 891163, 2022. https://doi.org/10.3389/fphy.2022.891163

[65] H. M. Ayaz, "Mixed convection in a driven cavity with an internal obstacle using the lattice Boltzmann method," *Therm. Sci.*, vol. 26, no. 6, pp. 5211–5226, 2022. https://doi.org/10.2298/TSCI220216109H

[66] K. Bouaraour and M. Lebbi, "Numerical investigation of hybrid nanofluid flow in a lid-driven cavity with a heated obstacle," *Proc. Rom. Acad. Ser. A*, vol. 25, no. 2, pp. 119–128, 2024. https://doi.org/10.59277/PRA-SER.A.25.2.06

[67] M. Y. Ali, M. A. Alim, and M. M. Karim, "Mixed convective heat transfer analysis by heatlines on a lid-driven cavity having heated wavy wall containing tilted square obstacle," *Math. Probl. Eng.*, vol. 2023, p. 1374926, 2023. https://doi.org/10.1155/2023/1374926

[68] M. Sannad, B. Abourida, and L. Belarche, "Numerical simulation of the natural convection with presence of the nanofluids in cubical cavity," *Math. Probl. Eng.*, vol. 2020, p. 8375405, 2020. https://doi.org/10.1155/2020/8375405

[69] M. K. Nayak, A. S. Dogonchi, and A. Rahbari, "Free convection of Al_2O_3-H_2O nanofluid inside a hexagonal-shaped enclosure with cold diamond-shaped obstacles and periodic magnetic field," *Case Stud. Therm. Eng.*, vol. 50, p. 103429, 2023. https://doi.org/10.1016/j.csite.2023.103429

[70] K. U. Rehman, W. Shatanawi, M. Zahri, E. S. M. Sherif, H. Junaedi, and Y. P. Lv, "Thermal analysis on

uniformly heated diamond obstruction in convective liquid suspension," *Case Stud. Therm. Eng.*, vol. 26, p. 101062, 2021. https://doi.org/10.1016/j.csite.2021.101062

[71] W. K. Hussam, K. Khanafer, H. J. Salem, and G. J. Sheard, "Natural convection heat transfer utilizing nanofluid in a cavity with a periodic side-wall temperature in the presence of a magnetic field," *Int. Commun. Heat Mass Transf.*, vol. 104, pp. 127–135, 2019. https://doi.org/10.1016/j.icheatmasstransfer.2019.02.018

[72] N. S. Gibanov and M. A. Sheremet, "Unsteady natural convection in a cubical cavity with a triangular heat source," *Int. J. Numer. Methods Heat Fluid Flow*, vol. 27, pp. 1795–1813, 2017. https://doi.org/10.1108/HFF-06-2016-0234

[73] M. Sannad, B. Abourida, and L. Belarche, "Numerical simulation of the natural convection with presence of the nanofluids in cubical cavity," *Math. Probl. Eng.*, vol. 2020, p. 8375405, 2020. https://doi.org/10.1155/2020/8375405

[74] H. F. Oztop, M. Mobedi, E. Abu-Nada, and I. Pop, "A heatline analysis of natural convection in a square inclined enclosure filled with a CuO nanofluid under non-uniform wall heating condition," *Int. J. Heat Mass Transf.*, vol. 55, pp. 5076–5086, 2012. https://doi.org/10.1016/j.ijheatmasstransfer.2012.05.007

[75] M. Sharifpur, T. Ntumba, and J. P. Meyer, "Parametric analysis of effective thermal conductivity models for nanofluids," in *Proceedings of the ASME 2012 International Mechanical Engineering Congress and Exposition*, Houston, Texas, USA, 2012, pp. 1–11. https://doi.org/10.1115/IMECE2012-85093

[76] R. L. Hamilton and O. K. Crosser, "Thermal conductivity of heterogeneous two-component systems," *Ind. Eng. Chem. Fundam.*, vol. 1, no. 3, pp. 187–191, 1962. https://doi.org/10.1021/i160003a005

[77] D. J. Jeffrey, "Conduction through a random suspension of spheres," *Proc. R. Soc. A*, vol. 335, pp. 355–367, 1973. https://doi.org/10.1098/rspa.1973.0130

[78] R. A. Arul Raja, J. Sunil, and R. Maheswaran, "Estimation of thermal conductivity of nanofluids using theoretical correlations," *Int. J. Appl. Eng. Res.*, vol. 13, no. 10, pp. 7932–7936, 2018.

Nomenclature

Be	Bejan number
C_p	Specific heat at constant pressure (J/Kg.K)
c	Location of the partition (m)
g	Acceleration duo to gravity (m/s^2)
Ha	Hartmann number (-)
h	Height of partition (m)
K	Thermal conductivity (W/m.K)
Ma	Marangoni number (-)
Nu	Nusselt number (-)
P	Pressure (N/m^2)
Pr	Prandtl number (-)
Ra	Rayleigh number (-)
T	Temperature (k)
t	Time (s)
u	The velocity component in x-direction (m/s)
v	The velocity component in y-direction (m/s)
w	The velocity component in z-direction (m/s)
x	The coordinate in horizontal direction (m)
y	The coordinate in vertical direction (m)
z	The coordinate in axial direction (m)

Greek symbols

α	Thermal diffusivity (m^2/s)
β	Coefficient of thermal expansion (K^{-1})
γ	Inclination angle of the magnetic field ($^\circ$)
θ	Lorentz force (-)
μ	Dynamic viscosity (Kg/m.s)
ρ	Density (Kg/m^3)
φ	Nanoparticles solid volume fraction (-)
Θ	Inclination angle of the cavity ($^\circ$)
ϕ	Inclination angle of the partition ($^\circ$)

Abbreviations

AR	Aspect Ratio
FDM	Finite Difference Method
FEM	Finite Element Method
FVM	Finite Volume Method
GFEM	Generalized Finite Element Method
LBM	Lattice Boltzmann Method
2D	Two-Dimensional
3D	Three-Dimensional
HT	Heat Transfer
HTR	Heat Transfer Rate
NC	Natural Convection

Subscripts

b	Block
c	Cold
D	Position of the hot source
E	External
eff	Effective
f	Fluid
I	Internal
L	Length
nf	Nano fluid
s	Solid particle